Arab J Sci Eng (2015) 40:3173–3185
DOI 10.1007/s13369-015-1791-x

RESEARCH ARTICLE - COMPUTER ENGINEERING AND COMPUTER SCIENCE

Multi-resolution MRI Brain Image Segmentation Based on Morphological Pyramid and Fuzzy *C*-mean Clustering

Hala Ali[1] · Mohammed Elmogy[1] · Eman El-Daydamony[1] · Ahmed Atwan[1]

Received: 25 February 2015 / Accepted: 13 July 2015 / Published online: 26 July 2015

Abstract Image segmentation is a vital step in many imaging applications, such as medical images and computer vision. Image segmentation is considered as a challenging problem, so we need to develop an efficient, fast technique for medical image segmentation. In this paper, we propose a new system for a multi-resolution MRI brain image segmentation, which is based on a morphological pyramid with fuzzy *C*-mean (FCM) clustering. In the first stage, we use a wavelet multi-resolution to maintain spatial context between pixels. Secondly, we use the morphological pyramid to fuse the resulting multi-resolution images with the original image to increase sharpness and decrease noise in the processed image. Finally, we use FCM technique to segment the processed images. We compared our proposed system with some state of the art segmentation techniques on two different brain data sets. Experimental results showed that the proposed system improves the accuracy of the MRI brain image segmentation.

Keywords Medical image segmentation · *k*-Means clustering (KM) · Expectation maximization (EM) · Fuzzy *C*-means (FCM) · Discrete wavelet transform (DWT) · Kernel fuzzy *C*-mean (KFCM_S2) · Morphological pyramid

✉ Mohammed Elmogy
elmogy@gmail.com; melmogy@mans.edu.eg

Hala Ali
Hala_ahmed703@yahoo.com

Eman El-Daydamony
Eman.8.2000@gmail.com

Ahmed Atwan
Atwan_2@yahoo.com

1 Department of Information Technology, Faculty of Computers and Information, Mansoura University, Mansoura, Egypt

1 Introduction

Segmentation can be defined as the operation of dividing images into constituent subregions. The result of image segmentation can be shown as a group of segments that collectively cover the whole image or a set of contours derived from the image. In some regions, the pixels can be classified according to some aspects or computed property, such as color, intensity, or texture. Adjacent regions are significantly different with respect to the same characteristic(s) [1]. The manual segmentation is possible, but it spends much time and subject to operator variability. There is a significant difficulty in reproducing a manual segmentation result due to the low level of confidence ascribed that we suffer accordingly. Therefore, automatic segmentation methods are preferable and are an active research area.

Segmentation of the brain magnetic resonance images (MRI) is currently considered as an active research topic in medical image processing. Segmentation of medical images can be divided into three main image problems. The first is the noise, which is contained in images by changing the intensity of the pixels [2]. The second is that the images exhibit the bias field (intensity inhomogeneity). It is induced by the radio frequency coil in MRI, and it is a big trouble in the computer-based analysis of MRI data. Finally, the partial volume effects where more than one tissue is inside a pixel volume [3]. There are many branches for image segmentation, such as texture analysis based methods, histogram thresholding-based methods, clustering-based methods, and region-based split and merging methods [4]. However, the image segmentation techniques are varied; it is so difficult to select an appropriate technique for a particular type of images. Not all techniques are suitable for all kinds of images [5].

Clustering algorithms are the most common used techniques of image segmentation. We can define clustering as an unsupervised learning technique, which needs the user to determine the number of clusters in advance to classify pixels [5]. As a result, the cluster is a collection of both similar pixels and dissimilar to the pixels belonging to other clusters [6]. There are two ways can be used in clustering algorithms: partitioning and grouping pixels [7]. In partitioning type, the whole image can be divided into smaller clusters in a successive way by the clustering algorithm, whereas in the grouping type, the algorithm starts with each element as a separate cluster and gathers them in successively larger clusters. The grouped pixels are based on some assumptions that decide how to arrange them preferably.

Several image segmentation methods are proposed and available for medical applications. These methods are chosen depending on the specific applications and different imaging modalities. Imaging problems, such as noise, partial volume effects, and motion, can also have significant consequences on the performance of the segmentation algorithms. Some of these methods, such as thresholding methods, region-growing methods, and clustering methods, were decried. Thresholding is considered as one of the main techniques of the medical image segmentation. It depends on separating pixels into different classes according to their gray levels. Thresholding approaches segment scalar images by creating a binary partitioning of the image intensities. The segmentation is then performed by groping all pixels with the intensity value greater than the threshold into one class and all other pixels into another class. The multi-thresholding process is the process in which more than one threshold values are determined. Its main restriction is that in its simplest form it deals only with two classes and it cannot be applied to multi-channel images [8,9]. In addition, thresholding does not typically take into consideration the spatial characteristics of an image. Therefore, it is susceptible to noise and intensity inhomogeneities, which can occur in MRI images.

In region-growing methods, the neighboring pixels are examined and added to a region class if no edges are detected in an approach. This process is repeated for each boundary pixel in the region. If there are adjacent regions, the weak edges are dissolved, and strong edges are left intact in an approach that is called a region-merging algorithm. Although, there are several advantages for region-growing methods over conventional segmentation techniques. Many disadvantages have appeared; for example, it is very computationally expensive. It takes both serious computing power (processing power and memory usage) and a decent amount of time to implement the algorithms efficiently [10].

Clustering methods can be defined as the process of assigning a set of observations into subsets (called clusters). Thus, observations in the same cluster are similar in some sense. Clustering can be considered as an unsupervised learning method [11]. Clustering can be done based on different attributes of an image such as size, color, and texture [12]. In clustering, we can classify either hard clustering or soft clustering. Hard clustering can be considered as a field in which a data item can belong to only one cluster, such as k-means clustering. On the other hand, soft clustering can be considered as a field in which a data item may belong to more than one cluster, such as FCM [13]. It is a confusing task to choose a proper clustering either hard or soft for a particular image whose properties will determine which one we will use [13].

In this paper, we focus on clustering techniques for medical image segmentation. We made our experiments by using the most used four clustering techniques: k-means, FCM, expectation maximization (EM), and kernel fuzzy C-means (KFCM_S2). This paper is divided into six sections as follows. In Sect. 2, we describe some fundamental concepts. Section 3 presents the current related work of some different medical image segmentation systems. In Sect. 4, we introduce the proposed system and discuss each stage in more detail. The experimental results and discussion of these results on two different benchmark data sets are described in Sect. 5. Finally, we present the conclusion and the future work in Sect. 6.

2 Basic Concepts

2.1 Wavelet

There are many types of multi-resolution image decomposition, such as Gaussian pyramids, Laplacian pyramids, and wavelets. Both the Gaussian and Laplacian representations need some necessary information to recover the original (full-resolution) image. These methods usually lead to a loss of information since the original image cannot be correctly reconstructed. Contrarily, the wavelet transform gives a complete image representation and doing decomposition according to both scale and orientation [14].

For creating a multi-resolution image, a Haar wavelet transform can be used [15]. The segmented low-resolution image is easily recovered to full-resolution (original image) by taking an inverse discrete wavelet transform. These functions are well localized in space and are, therefore, suitable for spatial domain analysis of signals and images. The continuous wavelet transform of functions $(t) \in L^2$ with respect to some analyzing wavelet ψ is defined as [14]:

$$C_{\psi}(b,a) = \int_{-\infty}^{\infty} s(t)\,\psi(t)\,\mathrm{d}t \tag{1}$$

where

$$\psi_{b,a}(t) = 1/\sqrt{a}\psi\left(\frac{t-b}{a}\right) \tag{2}$$

The parameters b and a are called shifting and scaling parameters, respectively. The normalization factor $a^{-1/2}$ is included so that $\|\psi_{b,a}\| = \|\psi\|$. Multi-resolution analysis of a signal $s(t)$ is done by using addition finite-energy function $\emptyset(t) \in L^2$, associated with ψ that is called a scaling function. Some properties of the ψ and $\emptyset$ are explained in the following equations [16]:

$$\int_{-\infty}^{\infty} \psi(t)\,\mathrm{d}t = 0, \quad \int_{-\infty}^{\infty} \emptyset(t)\,\mathrm{d}t = 1 \tag{3}$$

Consider a discrete signal at a particular scale A_0, the wavelet analysis of this signal gives two another signals (vectors) A_1 and D_1. The first signal is called an approximation and generated by the scaling function $\emptyset(t)$. It represents the signal A_0 that is averaged over some interval of length equal to the length of wavelet ψ and scaling function $\emptyset$ used in the analysis. Thus, A_1 represent A_0 at coarser resolution. The approximation gives information about slow changes in the signal because it contains only the low-frequency components of the signal. The other signal D_1 is called the details and generated by $\psi(t)$. It represents the details loss of A_0 in going from A_0 to A_1. The details contain the high frequency carried by the signal and not represent in A_1. It shows the rapid changes in the signal. Therefore, it can be easily used to discover the discontinuity points in the signal [17]. By repeating the analysis starting this time by A_1, we obtain a sequence of approximation A_l and details D_l, where l represents the level of analysis. The wavelet analysis can be extended from 1-D signal into images, which are considered as 2-D signals. It is necessary to represent the signal components by 2-D wavelet and a 2-D scaling function. Three different 2-D wavelets and one 2-D approximation function are constructed as follows [13]:

$$\psi^{[1]}i, j\,(x, y) = \emptyset(x-i)\,\psi(y-j) \tag{4}$$
$$\psi^{[2]}i, j\,(x, y) = \psi(x-i)\,\emptyset(y-j) \tag{5}$$
$$\psi^{[3]}i, j\,(x, y) = \psi(x-i)\,\psi(y-j) \tag{6}$$
$$\emptyset i, j\,(x, y) = \emptyset(x-i)\,\emptyset(y-j) \tag{7}$$

The 2-D wavelet analysis of an image gives four outputs (one approximation and three details): the approximation A, horizontal details H, vertical details V, and diagonal details D. The approximation A represents the image at a roughness resolution. It results from averaging in two directions of the images, x and y directions. The horizontal details H is obtained by taking averaging in x-directions and differencing the y-directions. The vertical details V is obtained by averaging in y-directions and differencing the x-directions. The diagonal details D can be obtained by taking the difference between two directions. Horizontal edges tend to show up in H, and vertical edges in while D contains all other details [18].

2.2 Morphological Pyramid

Image fusion is the operation of merging the relevant information from a set of images of the same scene to one image. Therefore, the result of image fusion will be more informative and complete rather than using a single image. Input images could be classified into multi-sensor, multimodal, multi-focal, or multi-temporal images. One of the goals of image fusion is to reconstruct a single improved image aiming the human visual perception, object detection, and target recognition [19]. Image fusion demands [20]: first, fused image should possess all possible relevant information contained in the source images; second, a fusion process should not present any artifact or unexpected feature in the fused image. Image registration can be considered as one of the important pre-procedures for the fusion process, i.e., the coordinate transformation of one image with respect to others. Image fusion algorithms can be classified into different levels: low, middle, and high; or pixel, feature, and decision levels. As shown in Fig. 1, there are various techniques for image fusion.

On the other hand, pyramid fusion algorithm is considered as a fusion method in the transform domain. In pyramid approach, we can obtain the pyramid levels by doing down sampling of source images that fused at the pixel level based on fusion rules. An image pyramid consists of a set of low-pass or band-pass copies of an image; each copy is to represent pattern information on a different scale. On each level of fusion, the pyramid would be divided into the half size of the previous pyramid and the higher levels will focus on the lower spatial frequencies [19].

2.3 Fuzzy *C*-Means Clustering (FCM)

FCM is an effective clustering algorithm that is developed in the 1970s by Dunn [21] and extended later by Bezdek [22] and Bezdek et al. [23]. Among the fuzzy clustering methods, FCM algorithm [24,25] is one of the most used image segmentation method because it has efficient characteristics for ambiguity.

Hard segmentation methods cannot maintain much information, such as soft segmentation methods spatially FCM. It has a serious limitation as does not incorporate any information about spatial context, which causes it to be suspect to noise and imaging artifacts. Fuzzy membership functions are used for assigns pixels to each class in FCM. Let $X = \{x_1, x_2, \ldots, x_N\}$ denotes an image with N pixels to be divided into c clusters [17]. The number of clusters is normally passed as an input parameter. Fuzzy partition of the given data set is carried out through the minimization of the objective function for a known number of clusters, subject

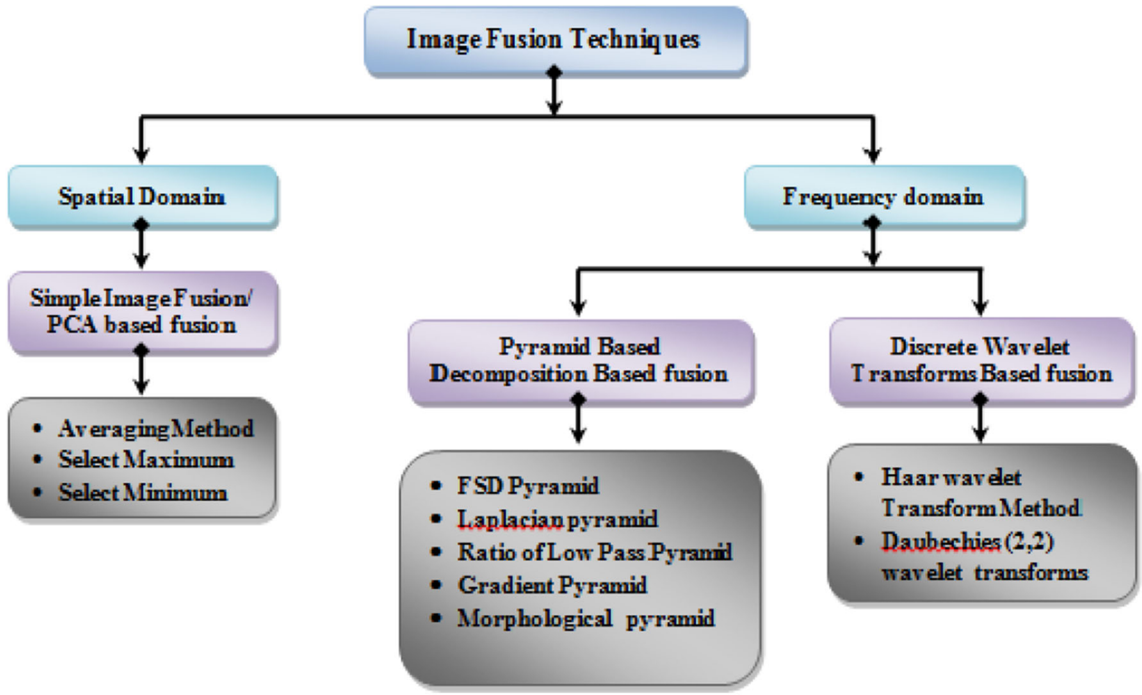

Fig. 1 The categorization of the image fusion techniques [19]

to the constraints that the sum of the membership grades of data in a cluster is 1. The FCM algorithm is based on the minimization of the following objective function [25].

$$J(U, V) = \sum_{i=1}^{c}\sum_{k=1}^{n} U_{ik}^{f} d_{ik}^{2} \tag{8}$$

where c is the number of cluster centroids or data subsets; n is the number of data points; m is the fuzzier value (1 for hard clustering, and increasing for fuzzy clustering); $d_{ik} = \|x_k - v_i\|^2$ is the Euclidean distance; x_k are the kth data points;v_i is the centroid of the ith cluster. U is the fuzzy partition matrix and V is the matrix of centroids of clusters. U_{ik} is the fuzzy membership value of pixel k in cluster i. This membership value satisfies the following constraints [24]:

$$0 \le U_{ik} \le 1, \quad \text{for} \quad 1 \le i \le c, 1 \le k \le n,$$
$$0 < \sum_{k=1}^{n} U_{ik} < n, \quad \text{for} \quad 1 \le i \le c,$$
$$\sum_{i=1}^{c} U_{ik} = 1, \quad \text{for} \quad 1 \le k \le n.$$

$$v_i = \sum_{k=1}^{n} (u_{ik})^f x_k \Big/ \sum_{k=1}^{n} (u_{ik})^f \tag{9}$$

$$u_{ik} = \left(\sum_{j=1}^{c} \left(\frac{d_{ik}}{djk}\right)^{2/(f-1)}\right)^{-1} \tag{10}$$

The termination criterion is as follows $\|U_{ik}^{(t+1)} - U_{ik}^{(t)} < \varepsilon$ where $\|.\|$ is the Euclidean norm and ε is a small number that can be set during the initialization process.

3 Related Work

Many researchers had exerted much effort to improve FCM algorithm performance for image segmentation. For example, Mostfa and Tolba [16] proposed an algorithm for segmenting a medical image by using a wavelet multi-resolution with EM algorithm, which is known as WMEM technique. In the first stage, they used Haar transform to detect spatial correlation between pixels with length 2. The second stage passed the original image and the two scaled version images generating form 2D Haar wavelet transform to EM algorithm to make segmentation separately. Then, they produced three segmented images each of them has weighted or thresholding value. Each pixel in the image is classified depending on these three segmented images.

Khalifa et al. [26] developed a system for segmenting MRI brain image based on wavelet and FCM (WFCM) algorithm. Their algorithm is robust and efficient approach to segmenting noisy medical images. Their proposed technique has two main stages: feature extraction and clustering. Feature extraction process is creating by using multi-level 2D wavelet decomposition features. Feature extraction from the wavelet decomposition is supplied to FCM for clustering. The images that obtain from the previous stage are segmented into three classes (WM, GM, and CSF) which are the brain tissue.

Bandhyopadhyay and Paul [27] proposed an efficient and fast way for diagnosis of the brain tumor. Their system consists of multiple phases. The first phase consists of registration of more than MR images of the brain taken on adjacent layers of the brain. In the second phase, they make a fusion between registered images to obtain a high-quality image for the segmentation. Finally, segmentation is performed by using improved k-means algorithm with dual-localization methodology.

Abdel Maksoud et al. [5] developed a medical image segmentation system based on hybrid clustering techniques to provide an accurate detection of brain tumor with minimal execution time. The clustering can be doing based on the integration between k-means and FCM or k-means and particle swarm optimization. In these systems, the main goal is to detect the brain tumor accurately in short execution time. They put into account the accuracy and minimum execution time in each stage. In the preprocessing stage, they applied the median filter to enhance the whole image quality and to remove the skull from the processed image. Both the processing time and the used amount of memory is reduced by this stage. In segmentation stage, all advantages of k-means, FCM, and particle swarm optimization are preserved, while their main troubles have been solved by the proposed integration techniques. A clear brain tumor clustering is presented by applying the thresholding. Finally, the level set stage is applied to give the contoured tumor area on the original image.

Parvathi [28] proposed a new segmentation algorithm for high-resolution remote sensing images, which can also be applied to medical and nonmedical images. They used a biorthogonal wavelet decomposition to describe a remote sensing image in multiple resolutions. A suitable resolution is chosen. The gradient image is estimated (or computed) by the simple grayscale morphology. To avoid over-segmentation, they have imposed the selective minima (regional minima of the image) on the gradient image. The watershed transform is applied, and the segmentation result is projected to a higher resolution, using the inverse wavelet transform until the full resolution of the segmented image is obtained.

Arakeri [29] proposed approach provides an efficient segmentation of brain tumor on MR images by using wavelet and modified FCM clustering. In the first phase, the image is decomposed by applying wavelet transform and in the next phase modified FCM algorithm is used to segment the approximate image in the highest wavelet level. Restraining noise and reducing the computational complexity of the process are performed by operating on a low-resolution image. Then the low-resolution segmented image is projected on to the full-resolution image by taking inverse wavelet transform.

Javed et al. [30] proposed a system comprising of two major phases, which involved a multi-resolution-based technique for noise removal and k-means technique for segmentation. Uncertainty and ambiguity are primary major issues of noise corrupted images and can lead to false segmentation. Therefore, multi-resolution-based noise removal is performed on the input image as a preprocessing step and then k-means-based technique is applied to the noise-free image to segment different objects present in image data automatically.

In this paper, the proposed system focus on improving the accuracy of medical image segmentation. Our system decreases the noise of MRI brain image, and a good-segmented image can be obtained without any misclassification. We present multi-resolution wavelet image fused by a morphological pyramid with FCM clustering. First, we use wavelet to utilize the spatial correlation between pixels. Second, we make a fusion between the original image and multi-resolution images or scaled version images to determine the noise pixel. We pass images to FCM to make segmentation to each of them. Finally, we compare FCM and KFCM with the proposed method.

4 The Proposed Segmentation System

In this section, we will discuss our proposed MRI brain tumor segmentation system that is called WMMFCM. The WMMFCM stand for wavelet multi-resolution (WM), morphological pyramid fusion (M), and fuzzy C-mean clustering (FCM) segmentation system. The proposed system introduces a new multi-resolution wavelet image fused by a morphological pyramid with FCM clustering technique. It is used to enhance the accuracy of the segmentation process. Soft segmentation methods, such as FCM, can keep much more information, but it cannot incorporate any information about spatial context. Therefore, we use discrete wavelet to solve this drawback of FCM [16,26].

As shown in Fig. 2, the proposed system consists of three major stages. The first stage is developed to create multi-resolution or multi-level 2D wavelet decomposition. In the second stage, we pass the three resulting images to the morphological pyramid to make a fusion between the original image and the two multi-resolution 2D Haar wavelet level. We create a fusion between the original image and the first-level image from DWT and although between the original image and the second-level 2D Haar wavelet transform. We get two new images in addition to the original image. In the last stage, we pass these three images to FCM clustering to make segmentation as shown in Fig. 5. In the sequent subsections, we will speak about the stages of our proposed system in more detail.

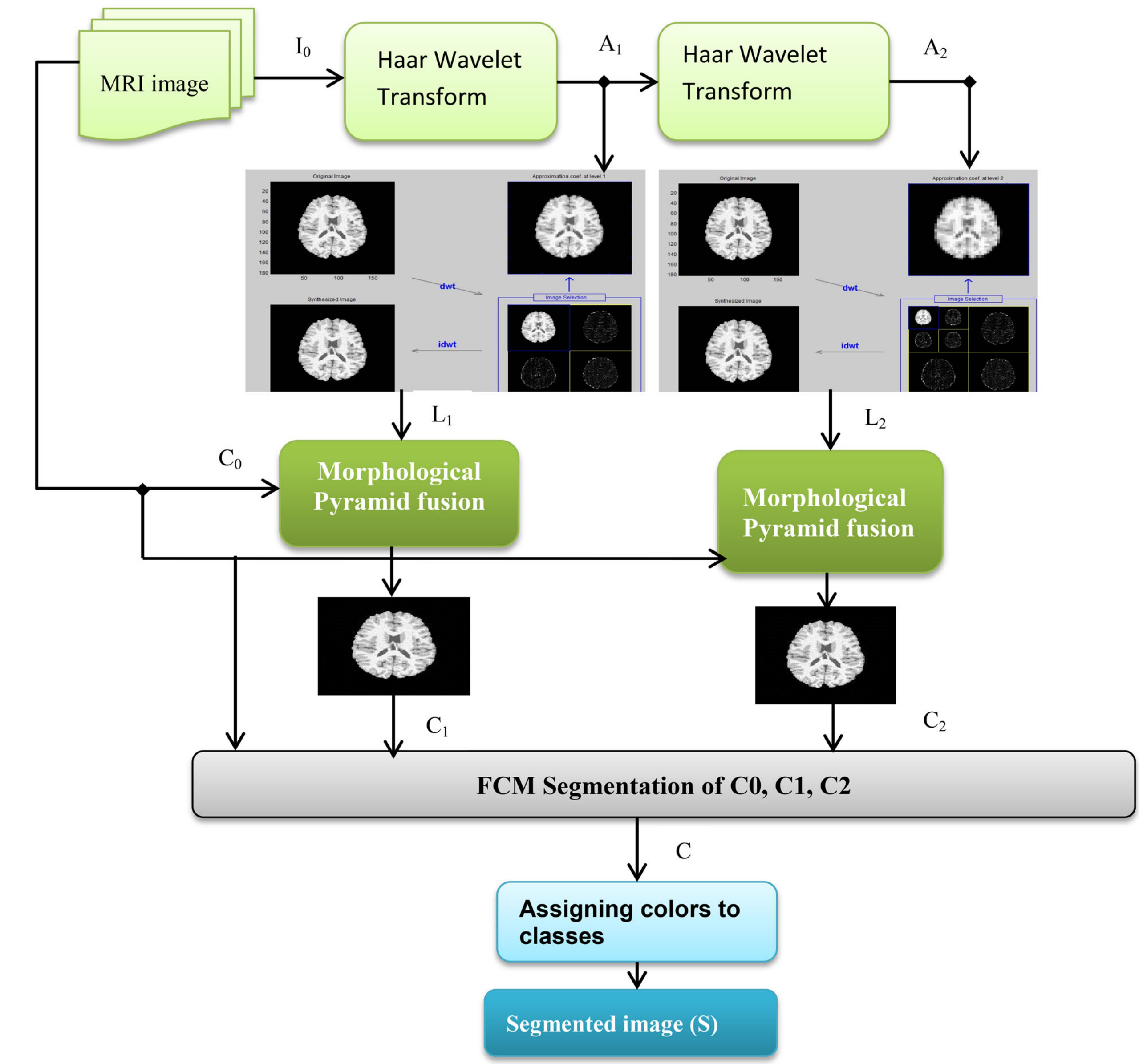

Fig. 2 The block diagram of the proposed WMMFCM System

4.1 Haar Wavelet Transform Stage

Multi-resolution analysis has been successfully used in image processing specially with image segmentation [31]. In this stage, we take the skull striped image as an input to 2D Haar discrete wavelet transform to apply multi-resolution to get the wavelet decomposition. Haar wavelet is applied to the image and performs a two-level wavelet transform. We get two outputs: low pass (approximation component) and high pass (detailed components). Then, we use the approximation component by taking inverse discrete wavelet transform (IDWT) to get the multi-resolution images [16]. The result of this stage is two multi-resolution images named with L_1 as level 1, and L_2 as level 2, as shown in Fig. 3.

4.2 Morphological Pyramid Fusion Stage

Morphological Pyramid Fusion works as the follows. First, considering a pair of input images. Second, the level of fusion of a pair of the input images of decomposition and recomposition should be determined. Third, in the decomposition, the input images are filtered at two levels, known as, open filtering and closed filtering. Fourth, the pair of images is decimated. Finally, the recomposition of the final fused image is obtained [32].

In this stage, we use the morphological pyramid to make a fusion between resulting images. We make fusion between the original image and the first-level image from 2D DWT and also between the original image and the second-level

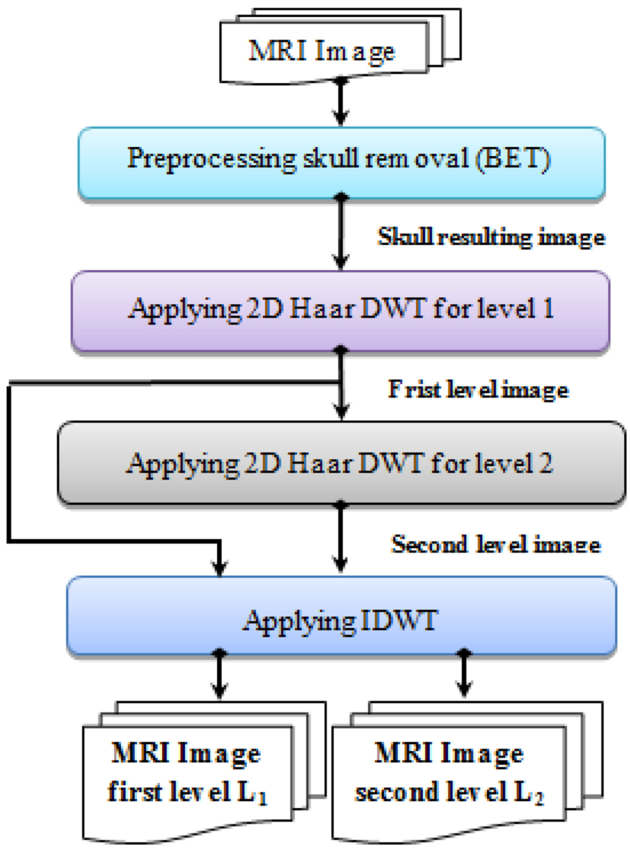

Fig. 3 The block diagram of the Haar and wavelet transform stage

2D Haar wavelet transform to get two new images in addition to the original image. In other words, the fusion process is performed between two pairs of images. The first pair is the original image (I0) and the first-level image from 2D DWT (L1). The second pair is the original image (I0) and the second-level image from 2D DWT (L2), as shown in Fig. 4. The level of the fusion (decomposition and recomposition) is decided to be level 1. The images are decimated to half the size, and the decomposition steps are iterated "Level" number of times. Both the decomposition part and the recomposition part are iteratively executed a "level" number of times. A morphological pyramid is obtained by performing filters to the image. The filter is usually for noise removal and image smoothing. It is similar to the effect of a low-pass filter, but it does not alter shapes and locations of objects in the image. The final fused image is obtained by making decimatation process between each of two pairs of images that are manipulated as one of the following, to produce final matrix by select maximum between pairs of images [32].

(a) Average between (I_0 & L_1) and (I_0 & L_2).
(b) Select maximum in between (I_0 & L_1) and (I_0 & L_2).
(c) Select minimum between (I_0 & L_1) and (I_0 & L_2).

In Haar wavelet transform, there is no need to increase the decomposition levels number because it may result in an overlap of neighboring features of the lower band signals. Hence, in morphological pyramid there is no need to increase the decomposition levels number because it does not produce good results. Although, we select the maximum in the process of decimated for image fusion to improve the sharpness.

4.3 FCM Stage

In this stage, we use FCM clustering [24] to segment the three resulting images from the previous stage. After we segment the three images, we passed the result of FCM clustering to the four conditions that control the final segmented image as shown in Fig. 5.

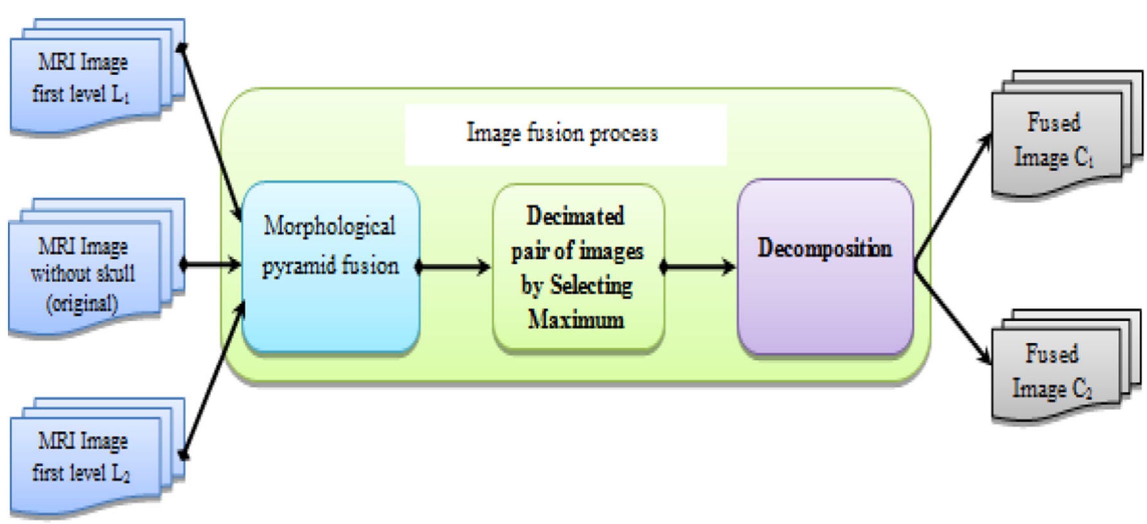

Fig. 4 The block diagram of the morphological pyramid stage

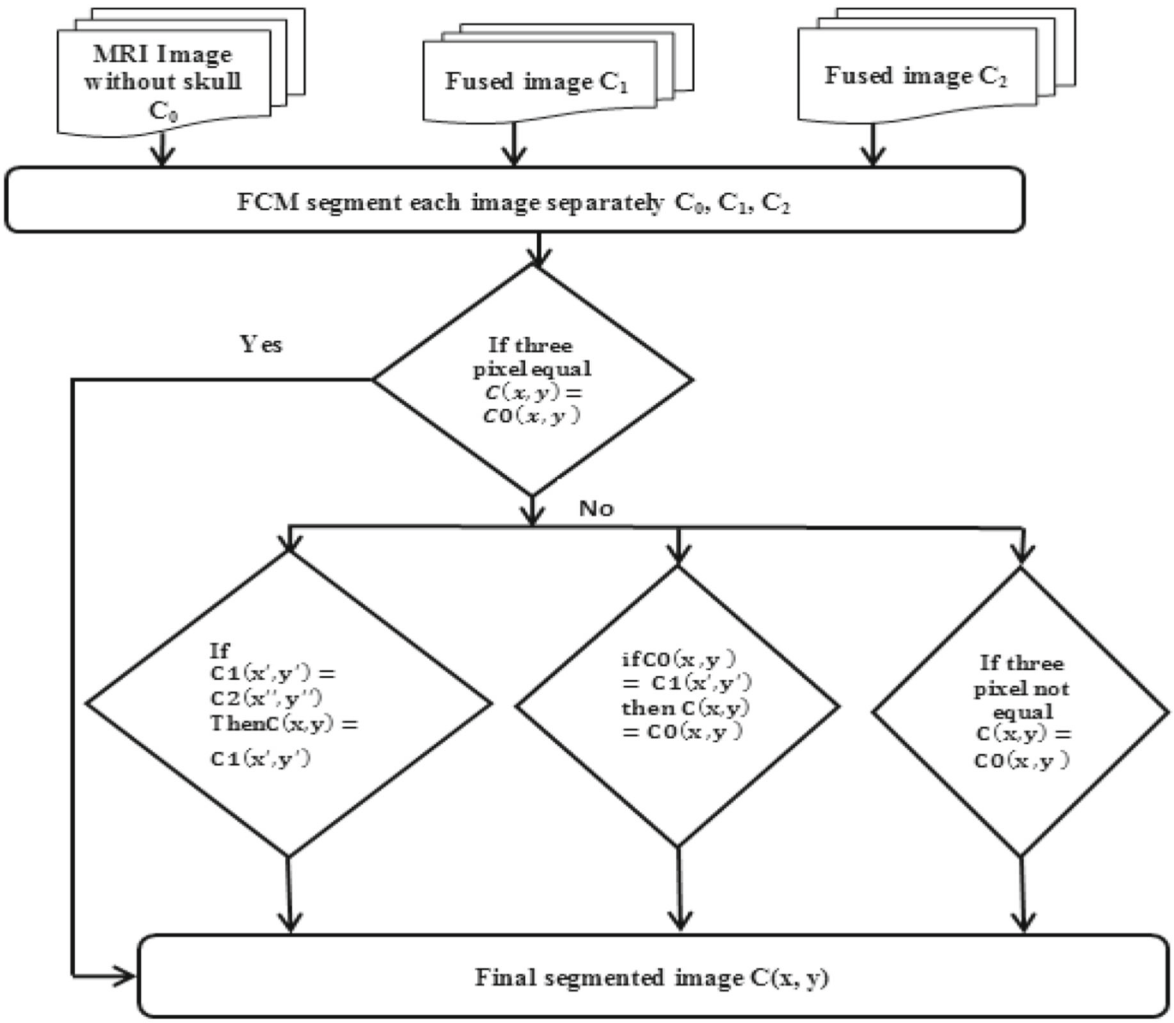

Fig. 5 The flowchart of the FCM technique

The image I_0, its child A_1, and grandchild A_2 pass through morphological pyramid fusion. We make a fusion between I_0, $L_{1,}$ and L_2. Then, they are passed through FCM algorithm for segmentation, which is used to segment each image independent from the others. This step gives three segmented images. In other words, it gives us three classification metrics C_0, C_1, and C_2. These three classification metrics reclassifies each pixel in the image I_0. Three points make the classification decision in the final segmented image. The three points are the choice of C that used to compute final segmented image as following:

1. if $C_0\,(x, y) = C1\left(x', y'\right) = C2\left(x'', y''\right)$ All the three pixel in C_0, C_1, C_2 belong to same class $then\ C\,(x, y) = C_0\,(x, y)$
2. if $C_1\left(x', y'\right) = C_2\left(x'', y''\right) \neq C_0\,(x, y)\ then\ C\,(x, y) = C_1\left(x', y'\right)$
3. if $C_0\,(x, y) = C_1\left(x', y'\right) \neq C_2\left(x'', y''\right)$ or if $C_0\,(x, y) = C_2\left(x'', y''\right) \neq C_1\left(x', y'\right)\ then\ C\,(x, y) = C_0\,(x, y)$
4. if $C_0\,(x, y) \neq C_1\left(x', y'\right) \neq C_2\left(x'', y''\right)\ then$ $C\,(x, y) = C_0\,(x, y)$ where $\left(x', y'\right)$ is the child, $\left(x'', y''\right)$ is grandchild of (x, y)

5 Experimental Results and Discussion

5.1 Dataset Description

In order to check the performance of our proposed image segmentation approach, the proposed algorithm is implemented in MATLAB R2011a on a Core$^{(TM)}$ 2 Due 2 GHz processor and 4 GB RAM. We used two benchmark datasets. The first is the Brain Web [33] database (DS1). It contains simulated brain MRI data based on normal and multiple sclerosis (MS). For both of these models, full three-dimensional data volumes have been simulated using three sequences [T1-, T2-, and proton-density- (PD-) weighted] and a variety of slice thicknesses, noise levels, and levels of intensity non-uniformity. It is T1 modality, 1-mm slice thickness, 3 %

Gaussian noises (calculated due to the brightest tissue) and 20 % intensity non-uniformity (RF). This dataset consists of 152 images. The second dataset is BRATS [34] database (DS2) from multimodal brain tumor segmentation. The dataset consists of multi-contrast MRI scans of 30 glioma patients (both low grade and high grade, and both with and without resection) along with expert annotations for “active tumor” and “edema.” For each patient, T1, T2, FLAIR, and post-Gadolinium T1 MRI images are available. This database has ground-truth images to compare the results of our method with them. This dataset contains 81 images. These images are obtained from Brain Web Database at the McConnell Brain Imaging Centre of the Montreal Neurological Institute, McGill University.

5.2 Measuring Segmentation Performance

The performance of our proposed system is measured by using the silhouette width, which measures the degree of confidence in the clustering assignment of a particular observation. Good-clustered observations have values near 1, and weakly clustered observations have values near −1. The silhouette width $s(i)$ of the object i can be calculated by [35]:

$$s\left(i\right)=\frac{b\left(i\right)-a\left(i\right)}{\max\left\{a\left(i\right),b\left(i\right)\right\}}\ (11) \tag{11}$$

where, $a(i)$ is the average distance between the ith data and all other data in the same cluster, and $b(i)$ is the smallest average distance between the ith data and all other data of other clusters [35]. The obtained silhouette accuracy of each method is listed in Table 6, 7, and 8.

A number of similarity coefficients are used to specify how well a given segment A matches a reference segment B, where A and B are sets of segmented pixels. The binary segmentation of the segmented image was compared with the reference image by calculating the number of correctly classified and misclassified voxel. The agreement of the binary segmentation with the reference was indicated by the following measures [36]:

1. Similarity index (SI) is a measure for the correctly classified voxel relative to the total area in both the reference and the area of the segmented image [36].

$$\mathrm{SI}=\frac{2\left(\mathrm{Ref}\cap\mathrm{Seg}\right)}{\mathrm{Ref}+\mathrm{Seg}}\times 100 \tag{12}$$

2. Correctly estimated percentage is a measure the area that is correctly classified voxel (overlap) relative to the area of the reference image [36].

$$\mathrm{PCE}=\frac{\mathrm{Ref}\cap\mathrm{Seg}}{\mathrm{Ref}}\times 100 \tag{13}$$

To test the effectiveness of the proposed method, we implemented and tested it by using two well-known brain datasets [33,34]. We use T1-weighted MRI for brain image that corrupted by noise. We used BET, which is freely available in the FMRIB FSL Software Library for skull stripping free software [37]. We implemented k-means, EM, FCM, KFCM, and our proposed method to make a comparison between them. The results showed that our proposed method superior to the other four tested algorithms. We segmented the image to three classes WM, GM, and CSF, as shown in Table 2. First, we made the skull stripping of the brain image by using BET. Second, we applied 2D multilevel to skull stripping image. Third, the fusion process was applied to images. Finally, different techniques were used with the proposed method for segmentation of the MRI brain images.

We can observe that the proposed method is more accurate than other tested techniques. There are two versions of KFCM: KFCM_S1 and KFCM_S2. We use KFCM_S2 which take median of the neighbors within the window aroundx_j. We use KFCM_S2 because it is more robust to the noise rather than using KFCM_S1 which take mean of the neighbors within the window aroundx_j. The parameter for KFCM_$S2$ $\alpha = 2$ and $\sigma = 50$ since σ is presented as a dispersion. Tables 1 and 2 describes each step of the proposed system for the two data sets. From Table 3, we can observe that the EM takes longer time than KM, but equal in accuracy as described in Tables 6, 7, and 8. In Table 3, it is noted that the KFCM takes long time but it is superior to the FCM in accuracy as shown in Tables 6, 7, and 8. In Tables 4 and 5, we use different level of noisy image for the two datasets. The proposed system is a good for dealing with noise as observed in Table 6. In Tables 6, 7, and 8, the performance is measured for each used technique.

6 Conclusion

Generally, medical images contain unknown noise. Therefore, it is hard to achieve acceptable performance for segmentation. Traditional FCM is one of the most used methods for medical image segmentation. It is not appropriate for dealing with noisy images because it is an intensity-based clustering algorithm. Although there were many extensions developed based on FCM, they cannot overcome the problem in a satisfied way. Therefore, an efficient multi-resolution MRI brain image segmentation technique is proposed, which is based on the morphological pyramid and FCM clustering. First, we used discrete wavelet to solve the drawbacks of FCM. Second, we used the morphological pyramid to detect spatially relevant information from the medical images. The results of cluster techniques are validated by using silhouette accuracy index, similarity index, and correctly estimated per-

Table 1 The first two stages of the proposed system by using WMMFCM applied on two benchmark data sets

Data Set	original	BET	Multi-resolution		Morphological Pyramid	
			DWTL1	DWTL2	Fused1	Fused2
DS1	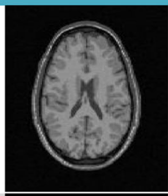					
DS2	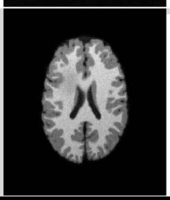	Already skull removed	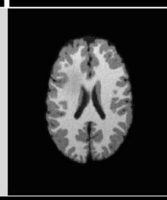	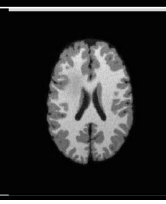	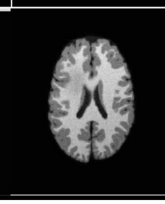	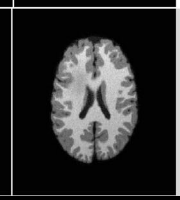

Table 2 The final stages of the proposed system by using WMMFCM applied on two benchmark data sets

DS1 set	WMMFCM			Truth/normal		
	WM	GM	CSF			
DS1			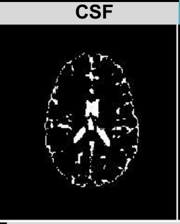	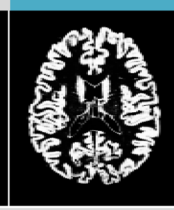		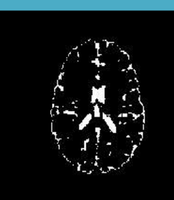
DS2						

Table 3 The comparison between KM and EM, FCM, and KFCM_ S2 clustering algorithms

	KM	Time	EM	Time	FCM	Time	KFCM_S2	Time
DS1	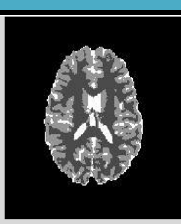	1.533303s	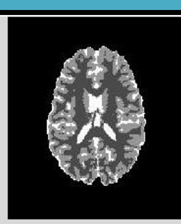	4.684700s	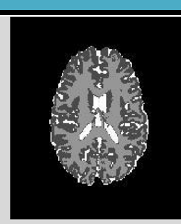	10.657680 s		11.6542107 s
DS2	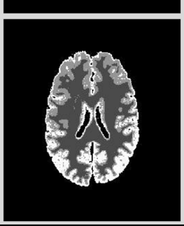	1.815886s	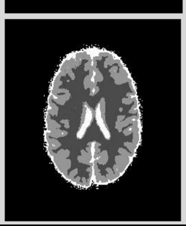	7.159113s		11.47670 s		14.326300s

Table 4 Our proposed system (WMMFCM) for segment with 3 % level of Gaussian noise

Dataset	Image 1 3% Noise 20% bias	Image 1 WMMFCM		
		White matter	Gray matter	CSF
DS1	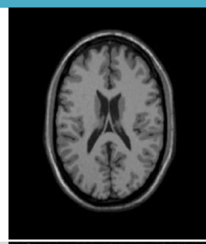	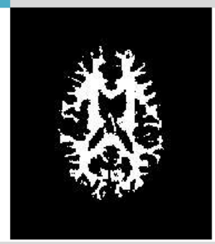	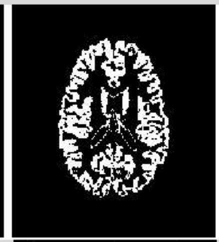	
DS2	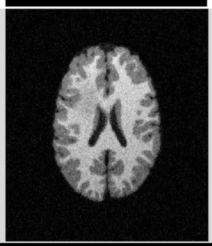		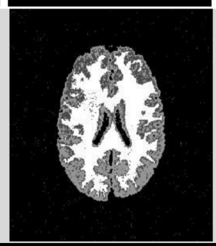	

Table 5 Our proposed system (WMMFCM) for segment with 5 % level of Gaussian noise

Dataset	Image 2 5% Noise 20% bias	Image 2 WMMFCM		
		White matter	Gray matter	CSF
DS1		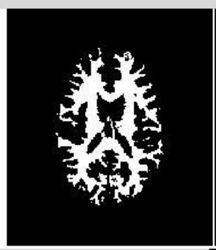		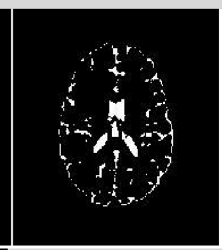
DS2	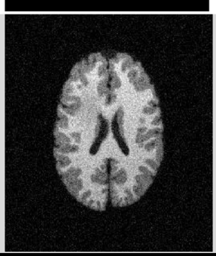		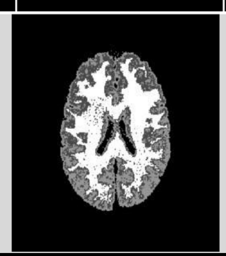	

centage. The proposed method is implemented and tested on a well-known two brain datasets. We used T1-weighted MRI for brain image that corrupted with noise. Results showed that the proposed method superior to KM, EM, FCM, and KFCM_S2. Image segmented into four classes WM, GM, CSF, and background.

In future, there are several ways to improve the overall segmentation performance. Noise is the challenging problem so that we work on this side to decrease noise or delete completely from the image. To decrease the noise of MR images, we will use different modalities or type of medical image of brain image such as CT and MRI with the proposed system. First, we use wavelet to get more than one level of the image. Second, we make a fusion between same levels from a different type of image. For example, we take the first-level DWT from MRI with the first-level DWT from CT and then fused them. Then, we will produce more than one image in addition to the original image.

Table 6 The comparison between KM, EM, FCM, KFCM, and our proposed system (WMMFCM) for dataset 1

Clustering techniques for DS1	Performance measure								
	SI			Silhouette value	Accuracy (%)	Time (s)	PCE		
	CSF	WM	GM				CSF	WM	GM
k-Means	91.87	89.120	90.005	0.9045	90.45	1.533303	90.001	90.612	89.65
EM	91.66	89.162	90.5	0.9050	90.50	4.684700	90.034	90.743	89.721
FCM	94.03	90.943	93.120	0.9567	95.67	10.657680	90.2021	88.654	92.98
KFCM_S2	95.01	90.012	92.03	0.9590	95.90	11.654210	93.87	91.5	94
WMMFCM	97.5	92.5	94	0.9705	97.05	11.83561	97.065	93.632	96

Table 7 The comparison between KM, EM, FCM, KFCM, and our proposed system (WMMFCM) for dataset 2

Clustering techniques for DS2	Performance measure								
	SI			Silhouette value	Accuracy (%)	Time (s)	PCE		
	CSF	WM	GM				CSF	WM	GM
k-Means	89.513	87.091	89.12	0.88503	88.503	1.815886	90.5	89.46	88.4
EM	89.520	87.067	89.12	0.88503	88.503	7.159113	90.5	89.46	88.04
FCM	94.42	89.23	93.120	0.9248	92.48	11.47670	89.656	90	91.6
KFCM_S2	94.765	89.67	91.05	0.9375	93.75	14.326300	93.5	92.3	93
WMMFCM	96.05	91.74	94.21	0.95853	95.853	13.03145	96.934	94	95.115

Table 8 The comparison between KM, EM, FCM, KFCM, and our proposed system (WMMFCM) for data set1 with different level of Gaussian noise

Clustering techniques for DS1	Performance measure for Image1 3 % Noise 20 % bias		Performance measure for Image2 5 % Noise 20 % bias	
	Silhouette value	Accuracy (%)	Silhouette value	Accuracy (%)
k-Means	0.8476	84.76	0.7823	78.23
EM	0.8490	84.90	0.7823	78.23
FCM	0.8856	88.56	0.83	83
KFCM_S2	0.90	90	0.8756	87.56
WMMFCM	0.9303	93.03	0.915	91.5

References

1. Begum, S.A.; Devi, O.M.: Fuzzy algorithms for pattern recognition in medical diagnosis. Assam Univ. J. Sci. Technol. **7**(2), 1–12 (2011)
2. Withey, D.J.; Koles, Z.J.: Medical image segmentation: methods and software. In: The Proceedings of Noninvasive Functional Source Imaging of the Brain and Heart and the International Conference on Functional Biomedical Imaging (NFSI&ICFBI), pp. 140–143 (2007)
3. Hou, Z.: A review on MR image intensity in homogeneity correction. Int. J. Biomed. Imaging **2006**, 1–11 (2006)
4. Ghamisi, P.; Couceiro, M.S.; Benediktsson, J.A.; Ferreira, N.M.F.: An efficient method for segmentation of images based on fractional calculus and natural selection. Expert Syst. Appl. **39**, 12407–12417 (2012)
5. Abdel Maksoud, E.; Elmogy, M.; Al-Awadi, R.M.: Efficient Hybrid Clustering Techniques for Brain Magnetic Resonance Image Segmentation. In: The Proceedings of the 2nd International Conference on Advanced Machine Learning Technologies and Applications (AMLTA14), Cairo, Egypt, Nov. 2014
6. Madhulatha, T.S.: An overview on clustering methods. Int. Organ. Sci. Res. J. Eng. **2**(4), 719–725 (2012)
7. Acharya1, J.; Gadhiya2, S.; Raviya, K.: Segmentation techniques for image analysis: a review. Int. J. Comput. Sci. Manag. Res. **2**(1), 1218–1221 (2013)
8. Ajala, A.F.; Oke, A.O.; Alade, M.O.; Adewusi, A.E.: Fuzzy K–C-means clustering algorithm for medical image segmentation. J. Inf. Eng. Appl. **2**(6), 21–32 (2012)
9. Zanaty, E.A.: Improved region growing method for magnetic resonance images (MRIs) segmentation. Am. J. Rem. Sens. **1**, 53–60 (2013)
10. Raju, P.D.R.; Neelima, G.: Image Segmentation by using histogram thresholding. Int. J. Comput. Sci. Eng. Technol. **2**(1), 776–779 (2012)
11. Kaur, N.; Kaur Sahiwal, J.; Kaur, N.: Efficient K-means clustering algorithm using ranking method in data mining. Int. J. Adv. Res. Comput. Eng. Technol. **1**, 85–91 (2012)

12. Acharya, J.; Gadhiya, S.; Raviya, K.: Segmentation techniques for image analysis: a review. Int. J. Comput. Sci. Manag. Res. **2**(1), 1218–1221 (2013)
13. Bora1, D.J.; Gupta, A.K.: Clustering approach towards image segmentation: an analytical study. Int. J. Res. Comput. Appl. Robot. **2**(7), 115–124 (2014)
14. Kim, J.; Kim, H.: Multiresolution-based watersheds for efficient image segmentation. Pattern Recognit. Lett. **24**, 473–488 (2003)
15. Priya, M.; Gobu, C.: A wavelet-based method for text segmentation in color images. Int. J. Comput. Appl. **69**(3), 14–17 (2013)
16. Mostfa, M.G.; Tolba, M.F.: Medical image segmentation using a wavelet-based multiresolution EM algorithm. In: IEEE International Conference on Industrial Electronics, Technology & Automation (2001)
17. Chuang, K.S.; Tzeng, H.L.; Chen, S.; Wu, J.; Chen, T.J.: Fuzzy C-means clustering with spatial information for image segmentation. Comput. Med. Imaging Graph. **30**, 9–15 (2006)
18. Kaiser, G.: The fast Haar transform: gateway to wavelet. IEEE Potent. Mag. **17**, 34–37 (1998)
19. Bedi, S.S.; Khandelwal, R.: Comprehensive and comparative study of image fusion techniques. Int. J. Soft Comput. Eng. **3**(1), 2231–2307 (2013)
20. Singh, R.; Khare, A.: Multiscale medical image fusion in wavelet domain. Sci. World J. **2013**, 1–10 (2013)
21. Dunn, J.C.: A fuzzy relative of the ISODATA process and its use in detecting compact well-separated clusters. J. Cybern. **3**, 32–57 (1974)
22. Bezdek, J.C.: A convergence theorem for the fuzzy data clustering algorithms. IEEE Trans. Pattern Anal. Mach. Intell. **2**, 1–8 (1980)
23. Bezdek, J.C.; Hall, L.O.; Clarke, L.P.: Review of MR image segmentation techniques using pattern recognition. Med. Phys. **20**, 1033–1048 (1993)
24. Yang, Y.: Image segmentation by fuzzy C-means clustering algorithm with a novel penalty term. Comput. Inform. **26**, 17–31 (2007)
25. Ramathilagam, S.; Pandiyarajan, R.; Sathy, A.: Modified fuzzy C-means algorithm for segmentation of T1–T2-weighted brain MR. J. Comput. Appl. Math. **235**, 1578–1586 (2011)
26. Khalifa, I.; Youssif, A.; Youssry, H.: MRI brain image segmentation based on wavelet and FCM algorithm. Int. J. Comput. Appl. **47**(16), 32–39 (2012)
27. Bandhyopadhyay, S.; Paul, T.: Automatic segmentation of brain tumour from multiple images of brain MRI. Int. J. Appl. Innov. Eng. Manag. **2**(1), 240–248 (2013)
28. Parvathi, K.; Rao, B.S.P.; Das, M.M.; Rao, T.V.: Pyramidal watershed segmentation algorithm for high-resolution remote sensing images using discrete wavelet transforms. Discrete Dyn. Nat. Soc. **2009**, 1–11 (2009)
29. Arakeri, M.P.; Reddy, G.R.M.: Efficient fuzzy clustering based approach to brain tumor segmentation on MR images. Commun. Comput. Inf. Sci. **250**, 790–795 (2011)
30. Javed, A.; Chai, W.Y.; Thuramaiyer, N.K.; Javed, M.S.; Alene, A.R.: Automated segmentation of brain MR images by combining contourlet transform and K-Means clustering techniques. J. Theor. Appl. Inf. Technol. **54**, 82–91 (2013)
31. AlZubi, S.; Islam, N.; Abbod, M.: Multiresolution analysis using wavelet, ridgelet, and curvelet transforms for medical image segmentation. Int. J. Biomed. Imaging **2011**, 1–18 (2011)
32. Uniyal, N.; Verma, S.K.: Image fusion using morphological pyramid consistency method. Int. J. Comput. Appl. **95**(25), 34–38 (2014)
33. Simulated Brain Database, McConnell Brain Imaging Centre, Montreal Neurological Institute, McGill University: http://www.bic.mni.mcgill.ca/brainweb. Accessed 27 Jun 2014
34. MICCA nice 2012: http://www2.imm.dtu.dk/projects/BRATS2012/data.html. Accessed 9 Aug 2014
35. Kannan, S.R.; Sathya, A.; Ramathilagam, S.; Devi, R.: Novel segmentation algorithm in segmenting medical images. J. Syst. Softw. **83**, 2487–2495 (2010)
36. He, R.; Datta, S.; Sajja, B.R.; Narayana, P.A.: Generalized fuzzy clustering for segmentation of multispectral magnetic resonance images. Comput. Med. Imaging Graph. **32**, 353–366 (2008)
37. FMRIB FSL Software Library: http://www.fmrib.ox.ac.uk/fsl/. Accessed 30 Dec 2011)